

## Neutrinoless Double-Beta Decay and Realistic Shell Model

Nunzio Itaco<sup>1,2,\*</sup>, Luigi Coraggio<sup>2</sup>, and Riccardo Mancino<sup>1,2</sup>

<sup>1</sup>Dipartimento di Matematica e Fisica, Università degli Studi della Campania “Luigi Vanvitelli”, viale Abramo Lincoln 5 - I-81100 Caserta, Italy

<sup>2</sup>Istituto Nazionale di Fisica Nucleare, Complesso Universitario di Monte S. Angelo, Via Cintia - I-80126 Napoli, Italy

**Abstract.** We report on the calculation of the neutrinoless double- $\beta$  decay nuclear matrix element for  $^{76}\text{Ge}$  within the framework of the realistic shell model. The effective shell-model Hamiltonian and the two-body transition operator describing the decay are derived by way of many-body perturbation theory. Particular attention is focused on the role played by the so-called Pauli blocking effect in the derivation of the effective operator.

### 1 Introduction

Neutrinoless double- $\beta$  ( $0\nu\beta\beta$ ) decay is an exotic nuclear process predicted by extensions of the Standard Model of particle physics. Observation of such a process would prove the non-conservation of lepton number, and show that neutrinos have a Majorana mass component (see Refs. [1, 2] and references therein).

In the framework of light Majorana neutrino exchange, the half life of the  $0\nu\beta\beta$  decay is inversely proportional to the square of the effective Majorana neutrino mass  $\langle m_\nu \rangle \equiv |\sum_i U_{ei}^2 m_{\nu_i}|$ . Explicitly, it can be written as

$$[T_{1/2}^{0\nu}]^{-1} = G^{0\nu} |M^{0\nu}|^2 \langle m_\nu \rangle^2, \quad (1)$$

where  $G^{0\nu}$  is the so-called phase-space factor (or kinematic factor), and  $M^{0\nu}$  is the nuclear matrix element (NME) directly related to the wave functions of the parent and grand-daughter nuclei. At present, the phase-space factors involved in the double  $\beta$  decays of nuclei of experimental interest are calculated with great accuracy [3, 4], therefore it is crucial to have precise values of the NME, both to improve the reliability of the  $0\nu\beta\beta$  lifetime predictions, and to extract neutrino properties from the experimental results.

Several nuclear structure models have been employed to provide NME values as precise as possible, the most largely employed being, at present, the Interacting Boson Model (IBM) [5–7], the Quasiparticle Random-Phase Approximation (QRPA) [8–11], Energy Density Functional methods [12], and the Shell Model (SM) [13–19].

Each model can be more suitable than another for a certain class of nuclei, and, when comparing the calculated NMEs, it can be seen that, at present, the results obtained with different approaches can differ by a factor of two or three (see for instance the review [20]).

It is worth noting that, all the above models are based on the use of a truncated Hilbert space to overcome the

computational complexity, but only within the realistic shell model an effective  $0\nu\beta\beta$  operator, which takes into account the degrees of freedom which do not appear explicitly in the calculated wavefunctions, may be introduced. This approach has been pioneered by Kuo and coworkers [21, 22], and more recently pursued by Holt and Engel [23]. Actually, in the SM approach it is possible to consider the correlations involving single-particle orbitals outside the model space deriving an effective operator. This is the so-called realistic shell-model approach where both the effective Hamiltonian and the transition operators are derived from a realistic free nucleon-nucleon ( $NN$ ) potential  $V_{NN}$  by way of the many-body theory [24, 25].

In two recent papers [26, 27], we have adopted the above approach to calculate properties related to the GT and  $2\nu\beta\beta$  decays of nuclei  $0\nu\beta\beta$ -candidates, with mass ranging from  $A = 48$  to  $A = 136$ . Our results and their comparison with the experimental data have shown that many-body perturbation theory (MBPT) allows to derive effective SM Hamiltonians and transition operators that reproduce quantitatively the observed spectroscopic and decay properties, without resorting to an empirical quenching of the axial coupling constant  $g_A$ .

On these grounds, we report in this paper on a preliminary calculation of the NME involved in the  $0\nu\beta\beta$  decay of  $^{76}\text{Ge}$ , that is currently investigated by GERDA experiment [28] at the Laboratori Nazionali del Gran Sasso (LNGS) of INFN, and by CDEX-1 experiment [29] at China Jinping Underground Laboratory.

Our theoretical framework is the many-body perturbation theory [25, 26, 30, 31]; we start from a realistic nuclear potential, and derive an effective SM Hamiltonian and a  $0\nu\beta\beta$  decay operator that are employed to calculate the wavefunctions of the ground states of  $^{76}\text{Ge}$  and  $^{76}\text{Se}$  and the  $0\nu\beta\beta$  NME. We focus our attention on the role of the so-called “blocking effect”, that takes into account the Pauli exclusion principle in systems with more than two

\*e-mail: nunzio.itaco@unicampania.it

valence nucleons [32, 33] in the derivation of the two-body effective  $0\nu\beta\beta$  operator.

The paper is organized as follows. In the next section we give a brief description of how we derive the shell-model Hamiltonian and the two-body effective  $0\nu\beta\beta$  decay operator. In Section 3, we report the results that we obtain for the  $^{76}\text{Ge}$  NME, analyzing in detail the contribution arising from the core-polarization blocking diagrams. A brief summary is reported in the last section.

## 2 Outline of calculations

The starting point of our calculation is provided by the high-precision CD-Bonn  $NN$  potential [34], that is smoothed integrating out its repulsive high-momentum components by way of the so-called  $V_{\text{low-k}}$  approach [35, 36]. In this way we get a softer  $NN$  potential defined up to a cutoff  $\Lambda$ , that preserves the physics of the original CD-Bonn interaction. The value of  $\Lambda$  is chosen, as in many of our recent papers [26, 27, 37–39] equal to  $2.6 \text{ fm}^{-1}$ , this value being a trade off between the need of minimizing the role of the missing three-nucleon force (3NF) [38] and that of ensuring the perturbative behavior of the potential. The Coulomb potential is explicitly taken into account in the proton-proton channel.

The harmonic oscillator (HO) potential  $U$  is introduced as an auxiliary one-body potential in order to break up the Hamiltonian for a system of  $A$  nucleons as the sum of a one-body term  $H_0$ , which describes the independent motion of the nucleons, and a residual interaction  $H_1$ :

$$\begin{aligned} H &= \sum_{i=1}^A \frac{p_i^2}{2m} + \sum_{i<j=1}^A V_{\text{low-k}}^{ij} = T + V_{\text{low-k}} = \\ &= (T + U) + (V_{\text{low-k}} - U) = H_0 + H_1 . \end{aligned} \quad (2)$$

It is now possible to define a truncated model space in terms of the eigenvectors of  $H_0$ . To study the  $0\nu\beta\beta$  decay of  $^{76}\text{Ge}$  we employ a model space spanned by the four  $1p_{3/2}, 1p_{1/2}, 0f_{5/2}, 0g_{9/2}$  proton and neutron orbitals outside the doubly-closed  $^{56}\text{Ni}$  core, and we derive an effective shell-model Hamiltonian  $H_{\text{eff}}$ , that takes into account the degrees of freedom that are not explicitly included in the shell-model framework.

We derive  $H_{\text{eff}}$  by resorting to the many-body perturbation theory, an approach that has been developed by Kuo and coworkers through the 1970s [24, 40]. More precisely, we use the well-known  $\hat{Q}$  box-plus-folded-diagram method [41], where the  $\hat{Q}$  box is defined as a function of the unperturbed energy  $\epsilon$  of the valence particles:

$$\hat{Q}(\epsilon) = PH_1P + PH_1Q \frac{1}{\epsilon - QHQ} QH_1P , \quad (3)$$

where the operator  $P$  projects onto the model space and  $Q = \mathbf{1} - P$ . In the present calculations the  $\hat{Q}$  box is expanded as a collection of one- and two-body irreducible valence-linked Goldstone diagrams up to third order in the perturbative expansion[31, 42].

Within this framework, it can be shown that the effective Hamiltonian  $H_{\text{eff}}$  can be written in terms of the  $\hat{Q}$  box derivatives [43]

$$\hat{Q}_m = \frac{1}{m!} \left. \frac{d^m \hat{Q}(\epsilon)}{d\epsilon^m} \right|_{\epsilon=\epsilon_0} , \quad (4)$$

$$H_{\text{eff}} = \sum_{i=0}^{\infty} F_i , \quad (5)$$

where

$$\begin{aligned} F_0 &= \hat{Q}(\epsilon_0) \\ F_1 &= \hat{Q}_1(\epsilon_0)\hat{Q}(\epsilon_0) \\ F_2 &= [\hat{Q}_2(\epsilon_0)\hat{Q}(\epsilon_0) + \hat{Q}_1(\epsilon_0)\hat{Q}_1(\epsilon_0)]\hat{Q}(\epsilon_0) \\ &\dots \end{aligned} \quad (6)$$

$\epsilon_0$  being the model-space eigenvalue of the unperturbed Hamiltonian  $H_0$ .

The  $H_{\text{eff}}$  for one-valence-nucleon systems provides the single-particle (SP) energies for our SM calculations, while the two-body matrix elements (TBMEs) are obtained from  $H_{\text{eff}}$  derived for the nuclei with two valence nucleons, by subtracting the theoretical SP energies.

The so obtained SP energies and TBMEs can be found in [27], where it is also reported a detailed discussion of the perturbative properties of  $H_{\text{eff}}$ .

The NME involved in  $0\nu\beta\beta$  decay,  $M^{0\nu}$ , may be expressed as

$$M^{0\nu} = M_{GT}^{0\nu} - \left(\frac{g_V}{g_A}\right)^2 M_F^{0\nu} \quad (7)$$

where the matrix elements are defined as follows:

$$M_{\alpha}^{0\nu} = \sum_{m,n} \langle 0_f^+ | \tau_m^- \tau_n^- O_{mn}^{\alpha} | 0_i^+ \rangle , \quad (8)$$

with  $\alpha = (GT, F)$ , having neglected the tensor term, whose effect has been estimated to be of the order of few percent [15]. The operators  $O_{mn}^{\alpha}$  have the following expression:

$$\begin{aligned} O_{mn}^{GT} &= \vec{\sigma}_m \cdot \vec{\sigma}_n H_{GT}(r) , \\ O_{mn}^F &= H_F(r) , \end{aligned}$$

and the neutrino potentials  $H_{\alpha}$  are defined using the closure approximation

$$H_{\alpha}(r) = \frac{2R}{\pi} \int_0^{\infty} f_{\alpha}(qr) \frac{h_{\alpha}(q^2)}{q + \langle E \rangle} G_{\alpha}(q^2) q dq , \quad (9)$$

where  $f_{F,GT}(qr) = j_0(qr)$ ,  $\langle E \rangle$  is the average energy of the virtual intermediate states used in the closure approximation, while the explicit expression of the form factors  $h_{\alpha}(q^2)$  can be found for instance in Ref. [44].

As mentioned before, we want to derive the effective  $0\nu\beta\beta$  decay operator tailored for the chosen model space. To this end, we resort to the formalism presented by Suzuki and Okamoto in Ref. [25]. In this approach, a non-Hermitian effective operator  $\Theta_{\text{eff}}$  can be expressed as

$$\begin{aligned} \Theta_{\text{eff}} &= (P + \hat{Q}_1 + \hat{Q}_1\hat{Q}_1 + \hat{Q}_2\hat{Q} + \hat{Q}\hat{Q}_2 + \dots) \\ &\quad \times (\chi_0 + \chi_1 + \chi_2 + \dots) . \end{aligned} \quad (10)$$

where the operators  $\chi_n$  are defined as:

$$\chi_0 = (\hat{\Theta}_0 + h.c.) + \hat{\Theta}_{00}, \quad (11)$$

$$\chi_1 = (\hat{\Theta}_1 \hat{Q} + h.c.) + (\hat{\Theta}_{01} \hat{Q} + h.c.), \quad (12)$$

$$\chi_2 = (\hat{\Theta}_1 \hat{Q}_1 \hat{Q} + h.c.) + (\hat{\Theta}_2 \hat{Q} \hat{Q} + h.c.) + (\hat{\Theta}_{02} \hat{Q} \hat{Q} + h.c.) + \hat{Q} \hat{\Theta}_{11} \hat{Q}, \quad (13)$$

...

where  $\hat{\Theta}_m, \hat{\Theta}_{mn}$  have the following expressions:

$$\hat{\Theta}_m = \frac{1}{m!} \left. \frac{d^m \hat{\Theta}(\epsilon)}{d\epsilon^m} \right|_{\epsilon=\epsilon_0}, \quad (14)$$

$$\hat{\Theta}_{mn} = \frac{1}{m!n!} \left. \frac{d^m}{d\epsilon_1^m} \frac{d^n}{d\epsilon_2^n} \hat{\Theta}(\epsilon_1; \epsilon_2) \right|_{\epsilon_1=\epsilon_0, \epsilon_2=\epsilon_0}, \quad (15)$$

with

$$\hat{\Theta}(\epsilon) = P\Theta P + P\Theta Q \frac{1}{\epsilon - QHQ} QH_1 P, \quad (16)$$

$$\hat{\Theta}(\epsilon_1; \epsilon_2) = PH_1 Q \frac{1}{\epsilon_1 - QHQ} Q\Theta Q \frac{1}{\epsilon_2 - QHQ} QH_1 P, \quad (17)$$

$\Theta$  being the bare transition operator.

It is worth noting that using Eqs. 5, 6, Eq. 10 may be then rewritten as

$$\Theta_{\text{eff}} = H_{\text{eff}} \hat{Q}^{-1} (\chi_0 + \chi_1 + \chi_2 + \dots), \quad (18)$$

enlightening the connection existing between the effective Hamiltonian and the effective operators.

In present calculation for the effective two-body  $0\nu\beta\beta$  decay operator, we arrest the  $\chi_n$  series to the  $\chi_2$  term. Since  $\chi_3$  depends on the first, second, and third derivatives of  $\hat{\Theta}_0$  and  $\hat{\Theta}_{00}$ , and on the first and second derivatives of the  $\hat{Q}$  box (see Eq. 13), our estimation of these quantities leads to evaluate  $\chi_3$  being at least one order of magnitude smaller than  $\chi_2$ . The calculation is performed starting from a perturbative expansion of  $\hat{\Theta}_0$  and  $\hat{\Theta}_{00}$ , and in Fig. 1 we report all the two-body  $\Theta_0$  diagrams up to the first order in  $V_{\text{low-k}}$ , the bare operator  $\Theta$  being represented by a dashed line.

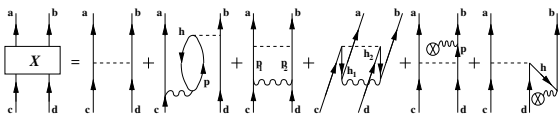


**Figure 1.** Two-body second-order diagrams included in the perturbative expansion of  $\hat{\Theta}$ . The dashed lines indicate the bare operator  $\Theta$ , the wavy lines the two-body potential  $V_{\text{low-k}}$ .

The circle with a cross inside represents a first-order ( $V_{\text{low-k}} - U$ )-insertion, arising from the  $U$  term in the interaction Hamiltonian  $H_1$  (see for example Ref. [31] for details).

The diagrams in Fig. 1 refer to the derivation of the effective operator for a system with two valence-nucleons. When dealing with nuclei with a larger number of valence nucleons, many-body diagrams come into play, accounting for the interaction via the two-body force of the many-valence nucleons with core excitations as well as with virtual intermediate nucleons scattered above the model space. The two topologies of second-order connected three-valence-nucleon diagrams for a two-body operator

$\hat{\Theta}$  are reported in Fig. 2 (diagrams (a) and (b)). These diagrams correct the Pauli-principle violation introduced by diagram (a<sub>1</sub>) and (b<sub>1</sub>) when one of the intermediate particle states is equal to  $m$ .

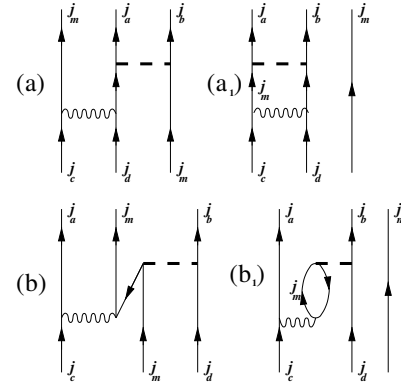


**Figure 2.** Three-body second-order diagrams that should appear in the perturbative expansion of  $\hat{\Theta}$ . As in Fig. 1, the dashed line indicates the bare operator  $\Theta$ , the wavy line the two-body potential  $V_{\text{low-k}}$ . For the sake of simplicity, for each topology only one of the diagrams which correspond to the permutation of the external lines is drawn.

Since there are no shell-model codes, at present, able to handle three-body transition operators, we derive a density-dependent two-body operator from the three-body one by summing and averaging over one incoming and outgoing particle of the connected diagrams (a) and (b) of Fig. 2. In this way we take into account the filling of the model-space orbitals when dealing with more than two valence nucleons.

More precisely, first we calculate exactly the three-body connected diagrams  $\langle [(j_a j_b)_J, j_m]_{J'} | (k) | [(j_c j_d)_J, j_n]_{J'} \rangle$ , with  $k$  equal to  $a$  and  $b$ , and whose expressions can be found in Ref. [45], then we evaluate the corresponding density-dependent two-body diagram  $\langle [(j_a j_b)_J] (k) | [(j_c j_d)_J] \rangle$ , whose explicit expression is

$$\langle [(j_a j_b)_J] (k) | [(j_c j_d)_J] \rangle = \sum_{m, J'} \rho_m \frac{j^2}{j^2} \langle [(j_a j_b)_J, j_m]_{J'} | (k) | [(j_c j_d)_J, j_m]_{J'} \rangle \quad (19)$$

where the summation over  $m$ -index runs in the model space, and  $\rho_m$  is the unperturbed occupation density of the orbital  $j_m$  accordingly to the number of valence nucleons.

The so obtained two-body contribution is finally added to the collection of the diagrams of the perturbative expansion of  $\hat{\Theta}$ .

### 3 Results

In this Section we present the results of our SM calculations for the NME of  $^{76}\text{Ge}$ . As previously mentioned, all

the calculations have been performed employing theoretical SP energies, TBMEs, and effective transition operators, describing  $^{76}\text{Ge}$  as a core of  $^{56}\text{Ni}$  plus 4 protons and 16 neutrons interacting in a reduced model space spanned by the four  $1p_{3/2}$ ,  $1p_{1/2}$ ,  $0f_{5/2}$ ,  $0g_{9/2}$  orbitals.

In Ref. [27] we have compared the calculated low-energy spectrum, the electromagnetic properties, the GT-strength distributions and the calculated NMEs of the  $2\nu\beta\beta$  decay with the available experimental data, showing a quantitative agreement.

In order to see how much the choice of the effective Hamiltonian can affect the value of the NME, in Table 1 we compare our calculated NME using the bare  $0\nu\beta\beta$  operator without any renormalization, with the values obtained in two other SM calculations performed using the same model space but with different empirical SM hamiltonians [15, 46].

**Table 1.** Theoretical  $0\nu\beta\beta$  NME calculated in the framework of the SM using different effective Hamiltonians. *I* and *II* are the results obtained by Menendez and coworkers [15] and by Sen'kov and coworkers [46], respectively. The  $0\nu\beta\beta$  operator employed is not renormalized.

	Our	I	II
NME	3.40	2.96	3.25

As it can be seen, the theoretical results are in good agreement, the largest discrepancy non exceeding 15%.

In Table 2 we report the calculated  $0\nu\beta\beta$  NME obtained using an effective operator derived by second order MBPT and taking into account all the intermediate states up to an excitation energy of  $14 \hbar\omega$ , which are enough to provide convergent NME values. To clarify the role of Pauli blocking diagrams we have derived two different operators with and without taking into account diagrams (a) and (b) of Fig. 2.

**Table 2.**  $M^{0\nu}$ ,  $M_{GT}^{0\nu}$  and  $M_F^{0\nu}$  for  $^{76}\text{Ge}$  calculated using the  $0\nu\beta\beta$  effective operator. See text for details.

	2nd	2nd + Pauli blocking
$M_{GT}^{0\nu}$	2.39	2.03
$M_F^{0\nu}$	-0.64	-0.66
$M^{0\nu}$	2.79	2.44

The inspection of Table 2 shows that including Pauli blocking diagrams provides a further reduction of  $M^{0\nu}$  by an amount around 10%, and that this effect is mainly due to the reduction of the Gamow-Teller contribution.

To better understand the action of Pauli blocking diagrams, we report in Table 3 the values of the diagrams reported in Fig. 2 for GT-operator corresponding to the most relevant configurations involved in the  $^{76}\text{Ge}$   $0\nu\beta\beta$  decay.

As expected, the density dependent diagrams (a) and (b) reduce the contribution of the Pauli violating diagrams (a<sub>1</sub>) and (b<sub>1</sub>).

**Table 3.** Values of the second-order diagrams reported in Fig. 2. The values of the diagrams (a) and (b) are calculated according to the expression in Eq. 19

$(j_a, j_b)_{J=0} (j_c, j_d)_{J=0}$	(a)	(a <sub>1</sub> )	(b)	(b <sub>1</sub> )
$(f_{5/2}, f_{5/2}) (g_{9/2}, g_{9/2})$	0.157	-0.337	-1.096	0.335
$(p_{3/2}, p_{3/2}) (g_{9/2}, g_{9/2})$	0.189	-0.263	-0.219	0.058

## 4 Summary

In this paper we have reported on some preliminary results for the SM calculation of the nuclear matrix element involved in the  $^{76}\text{Ge}$   $0\nu\beta\beta$  decay. The effective shell-model Hamiltonian and the two-body transition operator describing the decay are derived by way of many-body perturbation theory at third and second order, respectively. The role of the Pauli blocking three body diagrams that appear in the perturbative expansion of the effective operator when dealing with more than two valence nucleons, is taken into account in an approximate way by introducing two-body density-dependent diagrams.

## References

- [1] F.T. Avignone, S.R. Elliott, J. Engel, Rev. Mod. Phys. **80**, 481 (2008)
- [2] J.D. Vergados, H. Ejiri, F. Šimkovic, Rep. Prog. Phys. **75**, 106301 (2012)
- [3] J. Kotila, F. Iachello, Phys. Rev. C **85**, 034316 (2012)
- [4] S. Stoica, M. Mirea, Phys. Rev. C **88**, 037303 (2013)
- [5] J. Barea, F. Iachello, Phys. Rev. C **79**, 044301 (2009)
- [6] J. Barea, J. Kotila, F. Iachello, Phys. Rev. Lett. **109**, 042501 (2012)
- [7] J. Barea, J. Kotila, F. Iachello, Phys. Rev. C **87**, 014315 (2013)
- [8] F. Šimkovic, A. Faessler, V. Rodin, P. Vogel, J. Engel, Phys. Rev. C **77**, 045503 (2008)
- [9] F. Šimkovic, A. Faessler, H. Mütter, V. Rodin, M. Stauf, Phys. Rev. C **79**, 055501 (2009)
- [10] D.L. Fang, A. Faessler, V. Rodin, F. Šimkovic, Phys. Rev. C **83**, 034320 (2011)
- [11] A. Faessler, V. Rodin, F. Simkovic, J. Phys. G **39**, 124006 (2012)
- [12] T.R. Rodríguez, G. Martínez-Pinedo, Phys. Rev. Lett. **105**, 252503 (2010)
- [13] E. Caurier, F. Nowacki, A. Poves, Eur. Phys. J. A **36**, 195 (2008)
- [14] J. Menéndez, A. Poves, E. Caurier, F. Nowacki, Phys. Rev. C **80**, 048501 (2009)
- [15] J. Menéndez, A. Poves, E. Caurier, F. Nowacki, Nucl. Phys. A **818**, 139 (2009)
- [16] M. Horoi, Phys. Rev. C **87**, 014320 (2013)
- [17] M. Horoi, B.A. Brown, Phys. Rev. Lett. **110**, 222502 (2013)
- [18] A. Neacsu, M. Horoi, Phys. Rev. C **91**, 024309 (2015)
- [19] B.A. Brown, D.L. Fang, M. Horoi, Phys. Rev. C **92**, 041301 (2015)

- [20] J. Engel, J. Menéndez, *Rep. Prog. Phys.* **80**, 046301 (2017)
- [21] H.Q. Song, H.F. Wu, T.T.S. Kuo, *Phys. Rev. C* **40**, 2260 (1989)
- [22] A. Staudt, T.T.S. Kuo, H.V. Klapdor-Kleingrothaus, *Phys. Rev. C* **46**, 871 (1992)
- [23] J.D. Holt, J. Menéndez, A. Schwenk, *J. Phys. G* **40**, 075105 (2013)
- [24] T.T.S. Kuo, E. Osnes, *Lecture Notes in Physics*, vol. 364 (Springer-Verlag, Berlin, 1990)
- [25] K. Suzuki, R. Okamoto, *Prog. Theor. Phys.* **93**, 905 (1995)
- [26] L. Coraggio, L. De Angelis, T. Fukui, A. Gargano, N. Itaco, *Phys. Rev. C* **95**, 064324 (2017)
- [27] L. Coraggio, L. De Angelis, T. Fukui, A. Gargano, N. Itaco, F. Nowacki, *Phys. Rev. C* **100**, 014316 (2019)
- [28] M. Agostini, M. Allardt, E. Andreotti, A.M. Bakalyarov, M. Balata, I. Barabanov, M. Barnabé Heider, N. Barros, L. Baudis, C. Bauer et al. (GERDA Collaboration), *Phys. Rev. Lett.* **111**, 122503 (2013)
- [29] W. Zhao, Q. Yue, K.J. Kang, J.P. Cheng, Y.J. Li, S.T. Lin, Y. Bai, Y. Bi, J.P. Chang, N. Chen et al. (CDEX Collaboration), *Phys. Rev. D* **88**, 052004 (2013)
- [30] T.T.S. Kuo, J. Shurpin, K.C. Tam, E. Osnes, P.J. Ellis, *Ann. Phys. (NY)* **132**, 237 (1981)
- [31] L. Coraggio, A. Covello, A. Gargano, N. Itaco, T.T.S. Kuo, *Ann. Phys.* **327**, 2125 (2012)
- [32] P.J. Ellis, E. Osnes, *Rev. Mod. Phys.* **49**, 777 (1977)
- [33] I. Towner, *Physics Reports* **155**, 263 (1987)
- [34] R. Machleidt, *Phys. Rev. C* **63**, 024001 (2001)
- [35] S. Bogner, T.T.S. Kuo, L. Coraggio, *Nucl. Phys. A* **684**, 432c (2001)
- [36] S. Bogner, T.T.S. Kuo, L. Coraggio, A. Covello, N. Itaco, *Phys. Rev. C* **65**, 051301(R) (2002)
- [37] L. Coraggio, A. Covello, A. Gargano, N. Itaco, T.T.S. Kuo, *Phys. Rev. C* **91**, 041301 (2015)
- [38] L. Coraggio, A. Gargano, N. Itaco, *JPS Conference Proceedings* **6**, 020046 (2015)
- [39] L. Coraggio, A. Gargano, N. Itaco, *Phys. Rev. C* **93**, 064328 (2016)
- [40] T.T.S. Kuo, F. Krmpotić, K. Suzuki, R. Okamoto, *Nucl. Phys. A* **582**, 205 (1995)
- [41] T.T.S. Kuo, S.Y. Lee, K.F. Ratcliff, *Nucl. Phys. A* **176**, 65 (1971)
- [42] L. Coraggio, A. Covello, A. Gargano, N. Itaco, *Phys. Rev. C* **81**, 064303 (2010)
- [43] E.M. Krençiglowa, T.T.S. Kuo, *Nucl. Phys. A* **235**, 171 (1974)
- [44] R.A. Sen'kov, M. Horoi, *Phys. Rev. C* **88**, 064312 (2013)
- [45] A. Polls, H. Müther, A. Faessler, T.T.S. Kuo, E. Osnes, *Nucl. Phys. A* **401**, 124 (1983)
- [46] R.A. Sen'kov, M. Horoi, *Phys. Rev. C* **90**, 051301 (2014)